Inorganic Chemistry

ARTICLE

pubs.acs.org/IC

Ladder-Type *P,S*-Bridged *trans*-Stilbenes

Wannes Weymiens, Mark Zaal, J. Chris Slootweg, Andreas W. Ehlers, and Koop Lammertsma*

Department of Chemistry and Pharmaceutical Sciences, Faculty of Sciences, VU University Amsterdam, De Boelelaan 1083, 1081 HV Amsterdam, The Netherlands

Supporting Information

ABSTRACT: Phosphole-containing π-systems have emerged as building blocks with enormous potential as electronic materials because of the tunability of the phosphorus center. Among these, asymmetric *P*-bridged *trans*-stilbenes are still rare, and here an elegant and efficient synthesis toward such fluorescent molecular frameworks is described. Fine-tuning of the photophysical properties is attempted by enforcing the planarization of the phosphorus tripod and thus increasing the interaction between the phosphorus lone pair and the π-system. The electronic structure of the π-conjugated frameworks is analyzed with NMR, UV−vis and fluorescence spectroscopy, and time-dependent density functional theory (TD-DFT) calculations.

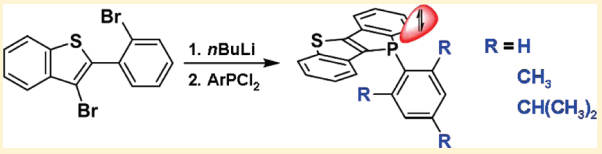

INTRODUCTION

Being neglected for decades, phosphorus has become of interest for π-conjugated molecular frameworks.[1] Especially the phosphole ring has shown potential as a building block for organic materials,[2] as exemplified by an organic light emitting device (OLED) based on dithienylphosphole gold chloride complex **1** (Figure 1).[3] The phosphole ring,[4] with its negligible degree of aromaticity, enables efficient conjugation over the diene moiety while offering a handle to fine-tune the photophysical properties of the π-system through the $\lambda^3\sigma^3$ phosphorus center. Recently, phospholes showed their potential in ladder-type (hetero)aromatic rings, such as the fused thiophene-phosphole-thiophene **2**[5] and the fused heterocycles **3a**−**d**[6] which can be viewed as a heteroatom-bridged *trans*-stilbene (Figure 1). The rigidity of such π-conjugated systems is known to enhance the luminescence intensity over flexible nonfused systems.[7] Introducing asymmetry by employing different heteroatom bridges in the same extended π-framework is the obvious next step to tune the electronic features. Only recently, systems that contain such an asymmetry are developed with, for example, *P,B*- and *P,C*-bridges in which the phosphole ring is either alkylated as in **3c**[6b] or oxidized as in **3d**.[6c]

Here we present a follow-up study on the very recently reported one on *P,S*-bridged *trans*-stilbenes bearing trans-fused benzo[*b*]phosphole and benzo[*b*]thiophene units[8] and report on their substituent-dependent photophysical properties. Whereas the tuning of these properties is often accomplished by chemical modification at the phosphorus center of the phosphole-containing π-system (e.g., oxidation, metal complexation, alkylation), we examine the effect of the degree in which the phosphorus lone pair participates in the π-conjugation. Namely, a pyramidal phosphorus in the phosphole ring implies an sp^3-type lone pair, which concurs with the negligible aromaticity, but planarizing this center should enhance the p-character of its lone pair and thus its participation in the π-framework.[9] To enforce planarization we increase the steric bulk of the substituent on phosphorus, thereby enlarging the C−P−C angles, by means of the phenyl, mesityl (Mes; 2,4,6-trimethylphenyl), and isityl (Is; 2,4,6-triisopropylphenyl) substituents.

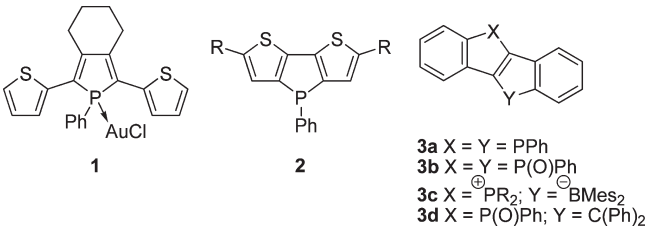

Figure 1. Selected phosphole-containing π-systems.

Scheme 1. Synthesis of *S,P*-Bridged *trans*-Stilbenes 6[a]

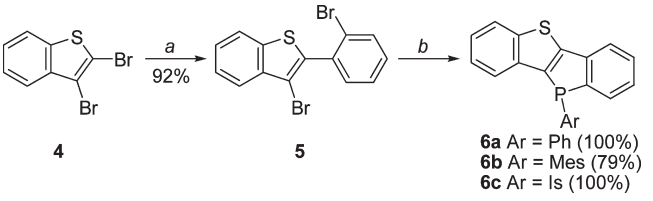

[a] (*a*) *o*-bromo-phenylboronic acid, $Pd(PPh_3)_4$, Na_2CO_3, 1,4-dioxane, H_2O, 100 °C, 16 h; (*b*) 1. *n*BuLi, Et_2O, −78 °C→RT, 2 h, 2. $ArPCl_2$, Et_2O, RT, 2−16 h.

RESULTS AND DISCUSSION

First we describe the synthesis of the *P,S*-bridged *trans*-stilbenes **6** with Ph, Mes, and Is as the phosphorus substituent.

Received: May 25, 2011
Published: July 27, 2011

Table 1. Spectroscopic Data for Phosphole-Containing π-Conjugated Systems 6a−c and 7a−c

compd	$\delta(^{31}P)^a$ (ppm)	$\lambda_{abs}{}^b$ (nm)	ε^b (M^{-1} cm^{-1})	$\lambda_{em}{}^c$ (nm)	$\Phi_F{}^c$	ss^d (cm^{-1})
6a	−17.4	316	1.80×10^4	411	0.253	5081
		340 (sh)	1.21×10^4			
6b	−29.7	310	4.64×10^4	408	0.121	4730
		343 (sh)	2.13×10^4			
6c	−33.4	324	1.66×10^4	409	0.154	4536
		345 (sh)	9.04×10^3			
7a	25.5	329	3.20×10^3	411	0.837	4078
		352 (sh)	2.77×10^3			
7b	27.4	329	3.33×10^3	408	0.895	3819
		353 (sh)	2.42×10^3			
7c	28.1	329	4.92×10^3	409	0.683	3023
		364 (sh)	2.57×10^3			

[a] ^{31}P NMR chemical shift in $CDCl_3$. [b] Absorption maximum in CH_2Cl_2 (10^{-5} M) and extinction coefficient. [c] Emission maximum and quantum yield in cyclohexane (10^{-6} M) using perylene (Φ_F = 94%) as standard. [d] Stokes shift.

Next, the influence of these substituents on the degree of planarizing the phosphorus center is examined by NMR, UV−vis, and fluorescence spectroscopy. These sections are followed by a computational analysis using density functional theory (DFT). Subsequently, the corresponding oxides **7** will be briefly discussed in the same manner.

Synthesis of *P,S*-Bridged *trans*-Stilbenes 6. We adapted the two-step synthetic route by Baumgartner et al.,[8] shown in Scheme 1, that is based on generating fused diarylphospholes from thiophenes.[5,10,11] The higher reactivity of the α-bromine of dibromobenzothiophene **4** is employed in a regioselective Suzuki coupling[12] with *ortho*-bromophenylboronic acid to give dibromide **5** in 92% yield after column chromatography (cf. lit. value of 73%).[8] The two bromine substituents of **5** are perfectly aligned for phosphorus introduction after lithiation with *n*BuLi. Quenching of dilithiated **5** with the appropriately substituted aryldichlorophosphine introduces the phosphorus fragment to give the known **6a** (100%) and the novel *P,S*-bridged *trans*-stilbenes **6b** (79%) and **6c** (100%), which were fully characterized spectroscopically.[13]

NMR Spectroscopy of 6. The ^{31}P NMR chemical shifts for **6a** (−17.4 ppm), **6b** (−29.7 ppm), and **6c** (−33.4 ppm) show a progressive shielding for the phosphorus nucleus with increase of the steric bulk of its substituent (Table 1). Whereas this effect might suggest a relationship with the hybridization of the phosphorus center, earlier calculations on phospholes have shown instead that an increase in phosphorus planarization, and thus an increase in electron delocalization, is more likely to cause a small downfield shift.[14] Hence, we attribute the ^{31}P-shielding to a sterically induced γ-effect of the phosphorus substituent's *ortho*-methyl and isopropyl groups in analogy to that reported for 1-isityl-3-methyl phosphole.[15]

The steric congestion caused by the alkyl groups of the aryl substituents of **6b** and **6c** is evident from their ^1H NMR spectra. Illustrative are the three sets of resonances that are observed for the isopropyl groups (^{i}Pr) of **6c**, which is the most congested of the three phospholes. Its *para*-substituent has chemical shifts ($\delta(^1H)$ = 2.90 ppm (CH); 1.29 ppm (CH_3)) in the expected range for aryl-^{i}Pr moieties, while one of the two *ortho*-substituents is significantly *deshielded* ($\delta(^1H)$ = 4.85 ppm (CH); 1.60/1.54 ppm (CH_3)) and the other one is *shielded* instead ($\delta(^1H)$ = 1.91 ppm (CH); 0.31/0.44 ppm (CH_3)). This difference between the two *ortho* ^{i}Pr groups is remarkable. We attribute the deshielding of one of the ^{i}Pr groups to the influence of the neighboring phosphorus atom and presume that the shielded ^{i}Pr group is located above the π-system. The two methyl groups of each *ortho* ^{i}Pr group are chemically inequivalent, have different chemical shifts, which suggests hindered rotation for the ^{i}Pr group, thereby underscoring the steric congestion of isomer **6c**. The same but less pronounced features are also present in the less crowded mesityl-substituted **6b**. Three different ^1H NMR methyl resonances are observed at 3.07, 2.25, and 1.26 ppm. The two *meta* protons of the mesityl group of **6b** resonate also at different chemical shifts (7.05 and 6.62 ppm). It is speculated that the upfield resonance is caused by the proton being in the shielding zone of the phosphole ring.

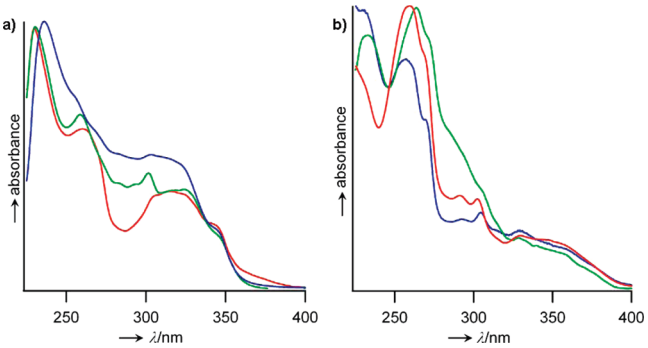

Figure 2. Absorption spectra in CH_2Cl_2 (10^{-5} M) of (a) phosphole-containing π-systems **6a** (red), **6b** (blue), and **6c** (green), and (b) their corresponding oxides **7a** (red), **7b** (blue), and **7c** (green).

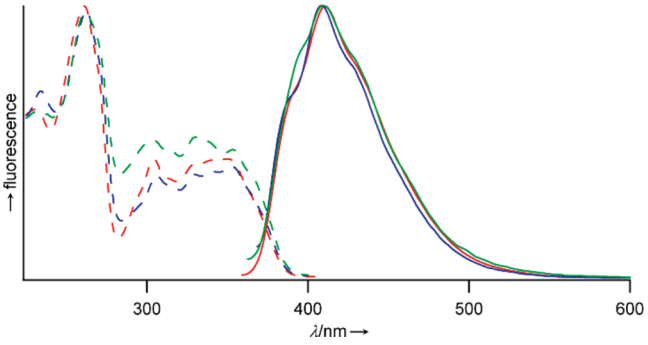

Figure 3. Fluorescence (solid) and excitation spectra (dotted) of **6a** (red), **6b** (blue), and **6c** (green) in cyclohexane (10^{-6} M; λ_{exc} = 350 nm; λ_{em} = 410 nm).

UV−vis and Fluorescence Spectroscopy of *P,S*-Bridged *trans*-Stilbenes 6. The absorption and fluorescence data of the phosphole-containing π-conjugated systems **6a−c** are summarized in Table 1. Two absorption maxima are observed at λ_{abs} = 258−260 nm and 316−326 nm with a shoulder 340−345 nm (Figure 2a). Excitation at either one of these absorptions results in a broad fluorescence band with a λ_{em} maximum at 408−411 nm (Figure 3) with quantum yields ranging from 0.121 to 0.253, which are higher than analogous phosphole-containing bridged *trans*-stilbenes (cf. Φ_F (**3a**) = 0.07;[6a] Φ_F (**3c**; R = cHex) = 0.02[6c]).

Increasing the substituent size on phosphorus causes a small bathochromic shift in the lowest energy absorption for **6**

dx.doi.org/10.1021/ic201116p |*Inorg. Chem.* 2011, 50, 8516–8523

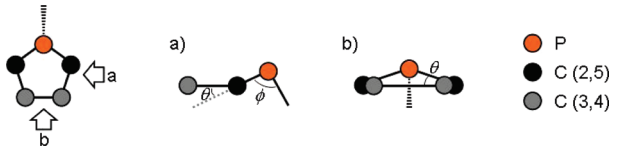

Figure 4. Deformations of the phosphole ring of the *P,S*-bridged *trans*-stilbenes **6**. Planarization of the P tripod is defined by angle ϕ and P out of C_4-plane bending by angle θ. (a) phosphole side view; (b) phosphole front view. For clarity, phosphole carbon atoms 2 and 5 are shown in black and carbons atoms 3 and 4 in gray.

(λ_{abs} (nm): **6a** 340; **6b** 343; **6c** 345), which suggests a decreasing gap between the highest occupied molecular orbital (HOMO) and the lowest unoccupied molecular orbital (LUMO). However, this trend is not reflected in the emission maxima (Figure 3), which all lie within 3 nm (λ_{em} (nm): **6a** 411; **6b** 408; **6c** 409). Thus, if there is a conjugative effect of the substituent size on the phosphorus lone pair participation in the π-system, this appears not to be reflected in the emission spectra of phospholes **6**. Puzzled by this apparent anomaly between the spectroscopic data, we next resorted to analyzing these data with theoretical means.

DFT Calculations of *P,S*-Bridged *trans*-Stilbenes 6. The electronic structures of the phosphole-containing π-systems **6a**−**c**, together with the sterically congested supermesityl substituted analogue **6d** (Ar = 2,4,6-tri-*tert*-butylphenyl (Mes*)),[13] were optimized using DFT with the OBPE functionals and the TZ2P basis set (see Computational Section). These calculations reveal two geometrical effects on increasing the size of the P-substituent. Most obvious are the enlarging C−P−C angles, Σ(∠P), causing flattening of the phosphorus, which is reflected in the angle ϕ between the P-substituent and the phosphole CPC plane (Figure 4; ϕ **6a** 114.2°, **6b** 123.1°, **6c** 125.0°, **6d** 129.8°). The consequence of the planarization is an enhanced interaction of the phosphorus lone pair with the carbon π-system. More subtle is the effect caused by the bulk of the substituent, which induces tilting of the phosphorus atom out of the plane formed by the four phosphole-carbon atoms. This dihedral angle θ (Figure 4) amounts to 6.2° for **6a** and increases to 9.6° for isityl-substituted **6c** (Table 2). As such, the phosphorus lone pair is tilted slightly toward a more parallel alignment with the carbon based π-orbitals, causing a better overlap.

Of interest are the frontier orbitals, because they may assist in analyzing the photophysical properties. To obtain insight into the influence of the phosphorus substituent on the frontier orbitals, we examined the forced planarization of the C_s-symmetry constrained **6a** in steps of approximately ten degrees.[16] This behavior is depicted in Figure 5, which shows that an increased planarization of the phosphorus tripod, as indicated by the sum of the three different C−P−C angles (Σ(∠P); range 290°−360°), pronouncedly affects the energy of the HOMO (ΔE_{HOMO} = 0.77 eV), but far less that of the LUMO (ΔE_{LUMO} = 0.14 eV). The result is a significantly reduced HOMO−LUMO energy gap for the planar analogue (ΔE_{HL} = 2.19 eV) when compared to the "pyramidal" one (ΔE_{HL} = 2.95 eV); the continuous decrease in ΔE_{HL} on planarizing the phosphorus fragment is evident in Figure 5 that gives the numerical values (in blue) above the Σ(∠P) *x*-axis. The relative HOMO and LUMO energies, and thus the ΔE_{HL} energies of the fully optimized **6a**, **6b**, **6c**, and **6d** nicely fit the pattern for the constrained planarization of **6a** (see the highlighted bars in Figure 4 with the numerical values in red). Hence, increasing the substituent size in the order phenyl (**6a**), mesityl (**6b**), isityl (**6c**), and supermesityl (**6d**) flattens the phosphorus center, leading to an increase in the energy of the frontier orbitals (see also Table 2).

On planarizing the phosphorus atom, its lone pair is expected to contribute more to the π-delocalized system, which is reflected in the contribution of the phosphorus 3p-orbital (3p(P)) in the HOMO. The effect for the stepwise planarization of **6a** is shown in the top of Figure 5. The equilibrium structures **6b**, **6c**, and **6d** have much enhanced 3p(P) participation to the HOMO of 22.5%, 25.1%, and 31.3%, respectively, as compared to **6a** (9.3%, Table 2). For the enforced fully planar system the contribution of the 3p(P) orbital to the HOMO amounts to 37.4%. Clearly, the 3p(P) component significantly affects the energy of the HOMO, but hardly that of the LUMO (Figure 5), causing a decrease in band gap and enhances π-conjugation with increasing substituent size.

The extent of conjugation appears to hardly influence the absorption maximum, as the bathochromic shift is only 5 nm in going from phenyl-substituted **6a** to isityl-substituted **6c**. This negligible effect can be attributed to the low probability of the HOMO→LUMO transition. Table 3 lists the time-dependent DFT calculated transitions visible in the absorption spectrum of **6a**. The transition associated for 74.3% with the HOMO→LUMO excitation (entry 1) has an oscillator strength (*f*) of only 0.08, while that for HOMO−1→LUMO (65.5%), mixed with HOMO→LUMO+2 (22.0%), (entry 3) has a much higher *f* of 0.13. This transition of 337.5 nm compares very well with the experimentally observed lowest energy absorption band at λ_{abs} = 340 nm. Since the HOMO−1 (ΔE_{HOMO-1} = 0.34 eV) and the LUMO (ΔE_{LUMO} = 0.21 eV) are less affected by planarization of the phosphorus tripod on going from **6a**−**d** than the HOMO (ΔE_{HOMO} = 0.48 eV; see Figure 5), the enhanced electronic interaction through the π-system has little effect on the photophysical properties.

Oxidized *P,S*-Bridged *trans*-Stilbenes 7. Electronic devices require fluorescent substances with high quantum yields, which the *P,S*-bridged *trans*-stilbenes **6a**−**c** do not have. Therefore the corresponding oxides **7a**−**c** were studied, as oxidation of the phosphorus center of rigid phosphole-containing π-systems generally enhances the fluorescence quantum yield, that is, Φ_F (**3a**) = 0.07 versus Φ_F (**3b**) = 0.98.[6a] The desired oxides **7a**−**c** were prepared in 37−47% yield by H_2O_2 treatment (Scheme 2),[17] as was recently shown to be successful for phenyl-derivative **7a**.[8]

Oxidation of the phosphorus center of **6a**−**c** leads to a significant deshielding of ^{31}P NMR chemical shift (42.9−61.5 ppm), which is caused by the electronegative oxygen atom. Interestingly, the trend in the relative chemical shifts for the phosphole oxides is reversed with the phenyl-substituted **7a** having the most shielded phosphorus atom; the differences in Δδ for **7a**−**c** are much smaller than for the nonoxidized forms (Table 1).

UV−vis and Fluorescence Spectroscopy of *P*(O),*S*-Bridged *trans*-Stilbenes 7. Oxidation of the phosphorus center of **6a**−**c** results in a bathochromic shift of the lowest energy absorption of 5−19 nm to λ_{abs} = 329 nm (max) and λ_{abs} = 352−364 nm (sh) (Figure 2b), suggesting that the HOMO−LUMO energy gap is reduced (Table 1).

Excitation of **7a**−**c** at either one of the two absorption bands results in a fluorescence band at λ_{em} = 408−411 nm (Figure 6), which is, in fact, at the same wavelength as that for the

Table 2. OPBE/TZ2P Computational Details for the Equilibrium Geometries of the Phosphole-Containing π-Conjugated Systems 6a−d

compd	$\Sigma(\angle P)^a$ (deg)	$E_{HOMO}{}^b$ (eV)	$E_{LUMO}{}^b$(eV)	$\Delta E_{HL}{}^c$ (eV)	3p(P)^d (%)	θ^e (deg)
6a	303.9	0.06	2.99	2.96	9.3	6.2
6b	316.0	0.29	3.14	2.85	22.5	8.7
6c	319.5	0.37	3.17	2.81	25.1	9.6
6d	324.8	0.54	3.20	2.66	31.3	6.7

[a] Sum of the C−P−C angles. [b] Relative HOMO and LUMO energies. [c] HOMO−LUMO gap. [d] 3p(P) contribution in the HOMO. [e] P bending out of the C_4-plane (Figure 4).

Table 3. Five Lowest-Energy Transitions Computed for 6a at TD-OPBE/TZ2P

entry	E^a (eV)	λ^b (nm)	f^c (a.u.)	main excitations (eV)^d (occurrence percentage)	
1	3.3895	365.8	0.0788	HOMO → LUMO (74.3)	HOMO → LUMO+1 (11.1)
2	3.4582	358.5	0.0257	HOMO → LUMO+1 (88.1)	HOMO → LUMO (8.2)
3	3.6733	337.5	0.1329	HOMO−1 → LUMO (65.5)	HOMO → LUMO+2 (22.0)
4	3.7690	329.0	0.0584	HOMO → LUMO+2 (63.3)	HOMO−1 → LUMO (11.8)
5	3.8240	324.2	0.0144	HOMO−1 → LUMO+1 (87.0)	HOMO−2 → LUMO (7.0)

[a] Transition energy. [b] Transition wavelength. [c] Oscillator strength. [d] Main excitations of the transition with relative contribution (see also Supporting Information, Table S3).

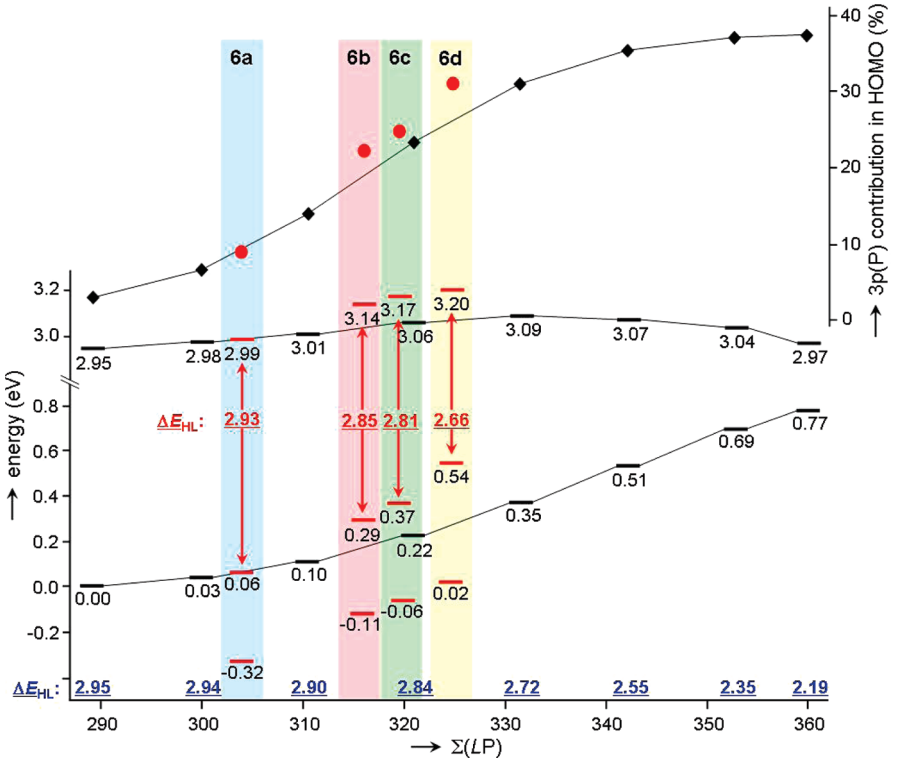

Figure 5. Relative OPBE/TZ2P HOMO and LUMO energies (in eV) on horizontal bars for constrained **6a** (black) and optimized **6a**−**d** (red) versus the sum of the C−P−C angles ($\Sigma(\angle P)$); the corresponding HOMO−LUMO gaps (ΔE_{HL}) are given in blue above the *X*-axes. For optimized **6a**−**d**, the HOMO−1 energy levels are given at the bottom of the graph. The 3p(P) contribution to the HOMO is given in the upper part of the graph with black squares for constrained **6a** and red dots for unconstrained **6a**−**d**.

corresponding $\lambda^3\sigma^3$-P analogues **6a**−**c**. Evidently, the bathochromic shift observed in the absorption upon oxidation is not transferred to the fluorescence. Hence, the Stokes shift is smaller for the oxidized species, meaning that less energy is lost during vibrational energy relaxation. What is different for the oxidized systems is the much higher quantum yield for fluorescence, that is, Φ_F = 0.683−0.895 for **7a**−**c** versus Φ_F = 0.121−0.253 for **6a**−**c**. Both the smaller Stokes shift and the higher quantum yield of the oxidized species can be rationalized by the better overlap of the wave functions of the S_0 and the S_1 state. Franck−Condon excitation then leads to a lower occupied vibrational level in the S_1 state and thus less relaxation is needed

dx.doi.org/10.1021/ic201116p |*Inorg. Chem.* 2011, 50, 8516–8523

Scheme 2. Oxidation of *S,P*-Bridged *trans*-Stilbenes 6a−c to the Corresponding Oxides 7a−c[a]

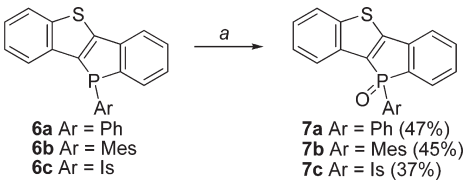

[a] *a*) H_2O_2, DCM, RT, 4−16 h.

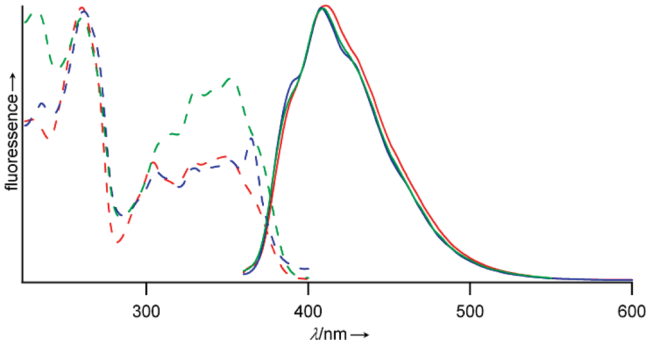

Figure 6. Fluorescence (solid) and excitation spectra (dotted) of phosphole-oxide-containing π-systems **7a** (red), **7b** (blue), and **7c** (green) in cyclohexane (10^{-6} M; λ_{exc} = 350 nm; λ_{em} = 410 nm).

to return to the vibrational S_1 ground state. Furthermore, a better overlap between the wave functions results in a higher probability of radiative decay and thus a higher quantum yield.

Whereas lone pair participation cannot play a role in the oxidized species **7a−c**, increasing the substituent size on phosphorus gives, like **6a−c**, a small bathochromic shift for the lowest energy absorption, that is, λ_{abs} **7a** = 352, **7b** = 353, and **7c** = 364 nm. In analogy with the nonoxidized species **6a−c**, this trend is not reflected in the emission maxima, which are at 408−411 nm within 3 nm of each other.

CONCLUSION

The P-substituted ladder-type *P,S*-bridged *trans*-stilbenes **6a−c** have been synthesized successfully. They exhibit intense emissions in the blue region (λ_{em} = 408−411 nm; Φ_F = 0.121−0.253). The influence of the size of the phosphorus substituent on the geometry and photophysical properties of the conjugated π-system was studied. DFT calculations revealed that increasing the bulkiness of the substituent results in a flattening of the pyramidal phosphorus, increased participation of its lone pair in the π-delocalization, and a decrease of the HOMO−LUMO gap. A larger contribution of the lone pair of phosphorus in the π-system raises the HOMO energy, while leaving the LUMO virtually unaffected. The more shielded ^{31}P NMR chemical shifts of the trigonal phosphorus nucleus of **6a−c** are attributed to steric influence of the more bulky substituents. Yet, these electronic effects are hardly expressed in the optical properties, apart from a small bathochromic shift of the lowest energy absorption as the substituent gets bigger. The reason is that the transition responsible for the lower energy absorption of **6a** is mainly associated with the HOMO−1→LUMO excitation.

The trigonal phosphorus centers could be oxidized with H_2O_2 to the corresponding *P*(O),*S*-bridged *trans*-stilbenes **7a−c**. These λ^5-phospholes exhibited significantly enhanced fluorescence quantum yields (Φ_F = 0.683−0.895), while the wavelengths for emission remain unaffected.

This study then shows that varying the steric bulk around the phosphorus center in extended *P,S*-containing π-frameworks affects the electronic properties of the nonoxidized **6a−c** and the oxidized **7a−c**. With the insight provided in this study we hope to have contributed to elucidating the intriguing photophysical properties of extended π-conjugated phosphole containing systems.

EXPERIMENTAL SECTION

Computational Details. All calculations were performed using the ADF program suite.[18] Geometries were optimized using the TZ2P basis set at the OBPE level of theory, using an integration accuracy of 5.0 and convergence criteria of 1×10^{-5}. An extensive description of the computational results for **6** and the calibration line, including frontier orbital pictures and coordinates, is given in the Supporting Information.

General Remarks. All reactions are carried out under nitrogen atmosphere using standard Schlenk techniques and dry solvents, unless stated otherwise. 1,4-Dioxane, tetrahydrofuran (THF), and Et_2O were distilled from Na/benzophenone, TEA from CaH_2, DCM from $CaCl_2$, and toluene from Na. Mesityl-dichlorophosphine[19] and 2,4,6-triisopropylphenyl-dichlorophosphine[20] were prepared according to literature procedures. 2,3-Dibromobenzo[*b*]thiophene (**4**) was prepared by a slightly modified literature procedure.[21]

NMR measurements were performed on a Bruker Advance 400 or a Bruker Advance 500. NMR chemical shifts were externally referenced to $SiMe_4$ (^{1}H and ^{13}C) or 85% H_3PO_4 (^{31}P). IR spectra were recorded on a Shimadzu FTIR-8400S, and high-resolution mass spectra were measured on a Bruker micrOTOF-Q (ESI) or a JEOL LMS-SX/SX 102 A tandem mass spectrometer (FAB). UV−vis spectra are recorded at room temperature on a Carey 300 UV−visible spectrophotometer and fluorescence spectra on a Perkin-Elmer LS50-B luminescence spectrometer. Spectra were recorded with a scan speed of 200 nm/min, using a spectral width of 5 nm for both excitation and emission. Quantum yields were determined as 10^{-6} M cyclohexane solutions, using perylene as standard (Φ_F = 94%).

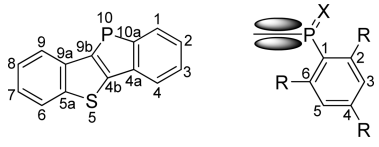

2,3-Dibromobenzo[*b*]thiophene (4).[21] NBS (46.4 g, 260 mmol, 2.5 equiv) was added in small portions over a period of 1 h to a solution of benzo[*b*]thiophene (14.0 g, 104 mmol, 1 equiv) in DCM/acetic acid (1/1 (v/v), 820 mL) at 0 °C. The color of the reaction mixture changed from yellow to red and stirring was continued at room temperature. The progress of the reaction was checked by aqueous workup of small aliquots of the reaction mixture. To speed up the reaction, three portions of NBS were added to the reaction mixture at t = 17 h (18.5 g, 104 mmol), t = 89 h (5.56 g, 31.2 mmol), and at t = 5 days (4.26 g, 23.9 mmol). After 8 days of stirring, the reaction mixture was washed subsequently with 10% KOH (aq), 5% $NaHCO_3$ (aq), 5% $Na_2S_2O_3$ (aq), and water. The organic phase was dried over $MgSO_4$, filtered, and all volatiles were removed in vacuo. The yellow residue was subjected to column chromatography over silica gel eluting with hexane

dx.doi.org/10.1021/ic201116p |*Inorg. Chem.* 2011, 50, 8516–8523

to obtain **4** as a white solid (24.8 g, 84.8 mmol, 82%). ^{1}H NMR ($CDCl_3$; 250.13 MHz): δ (ppm) = 7.74 (d, $^3J_{HH}$ = 7.4 Hz, 1H, H^4); 7.73 (dd, $^3J_{HH}$ = 7.1 Hz, $^4J_{HH}$ = 1.5 Hz, 1H, H^7); 7.43 (dt, $^3J_{HH}$ = 7.6 Hz, $^4J_{HH}$ = 1.5 Hz, 1H, H^5); 7.38 (dt, $^3J_{HH}$ = 7.0 Hz, $^4J_{HH}$ = 1.4 Hz, 1H, H^6).

3-Bromo-2-(2-bromophenyl)benzo[*b*]thiophene (5). 2,3-Dibromobenzo[*b*]thiophene (2.13 g, 7.34 mmol, 1 equiv), 2-bromophenyl boronic acid (1.47 g, 7.34 mmol, 1 equiv), and $Pd(PPh_3)_4$ (424 mg, 367 μmol, 5 mol %) were dissolved in 1,4-dioxane (75 mL), and degassed 2 M Na_2CO_3 (aq; 15 mL) was added. The yellow reaction mixture was refluxed for 16 h, after which the solvent was removed. The residue was redissolved in DCM and washed with water. The organic layer was dried over $MgSO_4$, filtered, and the solvent was removed in vacuo. The yellow residue was purified by column chromatography over silica gel eluting with hexane (R_F = 0.26) and resulted in **5** as a white solid (2.48 g, 6.74 mmol, 92%). Mp: 72.5−73.3 °C. ^{1}H NMR ($CDCl_3$; 400.13 MHz): δ (ppm) = 7.88 (dd, $^3J_{HH}$ = 7.8 Hz, $^4J_{HH}$ = 1.4 Hz, 1H, H^4); 7.84 (dd, $^3J_{HH}$ = 7.8 Hz, $^4J_{HH}$ = 1.1 Hz, 1H, H^7); 7.73 (dd, $^3J_{HH}$ = 8.0 Hz, $^4J_{HH}$ = 1.1 Hz, 1H, $H^{6'}$); 7.50 (dt, $^3J_{HH}$ = 7.8 Hz, $^4J_{HH}$ = 1.1 Hz, 1H, H^5); 7.45 (dd, $^3J_{HH}$ = 7.4 Hz, $^4J_{HH}$ = 2.0 Hz, 1H, $H^{3'}$); 7.44 (dt, $^3J_{HH}$ = 7.8 Hz, $^4J_{HH}$ = 1.4 Hz, 1H, H^6); 7.42 (dt, $^3J_{HH}$ = 7.4 Hz, $^4J_{HH}$ = 1.1 Hz, 1H, $H^{4'}$); 7.33 (ddd, $^3J_{HH}$ = 8.0 Hz, $^3J_{HH}$ = 7.4 Hz, $^4J_{HH}$ = 2.0 Hz, 1H, $H^{5'}$). ^{13}C NMR ($CDCl_3$; 62.90 MHz): δ (ppm) = 138.4 (s, C^{7a}); 137.8 (s, C^{3a}); 137.2 (s, $C^{1'}$); 134.1 (s, C^2); 133.0 (s, $C^{6'}$); 132.5 (s, $C^{3'}$); 130.6 (s, $C^{5'}$); 127.1 (s, $C^{4'}$); 125.6 (s, C^6); 125.2 (s, C^5); 124.5 (s, $C^{2'}$); 123.6 (s, C^4); 122.2 (s, C^7); 108.5 (s, C^3). HR-MS (FAB): calcd for $C_{14}H_8{}^{79}Br^{81}BrS$: 367.8693, found: 367.8695. *m*/*z* (%): 370 (54) [M ($^{81}Br)_2]^+$, 368 (100) [M ($^{79}Br^{81}Br$)]$^+$, 366 (50) [M ($^{79}Br)_2]^+$, 208 (40) [M − $Br_2]^+$. IR (neat): ν (cm^{-1}) = 3067 (w); 1462 (m); 1433 (m); 1420 (m); 1321 (w); 1308 (w); 1254 (m); 1051 (w); 1018 (m); 976 (w); 887 (m); 799 (w); 746 (s); 727 (m); 683 (m); 644 (w); 621 (w); 584 (w); 500 (w); 444 (m).

10-Phenyl-10*H*-benzo[*b*]phosphindolo[2,3-*d*]thiophene (6a). *n*-BuLi (1.6 M in hexane, 2.75 mL, 4.40 mmol, 2.2 equiv) was added dropwise over a period of 45 min to a solution of 3-bromo-2-(2-bromophenyl)benzo[*b*]thiophene (737 mg, 2.00 mmol, 1 equiv) in Et_2O (40 mL) at −78 °C. The reaction mixture was stirred for 30 min at −78 °C and was then slowly warmed to room temperature over a period of 1.5 h. $PhPCl_2$ (270 μL, 2.00 mmol, 1 equiv) was slowly added dropwise to the light yellow turbid reaction mixture over a period of 30 min. Stirring was continued for 3 h, during which the reaction mixture turned slightly darker. The solvent was removed in vacuo, and the residue was extracted into Et_2O. After removal of the solvent in vacuo, the crude product was purified by column chromatography over Al_2O_3 eluting with DCM (R_F = 0.65), which resulted in **6a** as a yellow solid (632 mg, 2.00 mmol, 100%). ^{1}H NMR ($CDCl_3$; 400.13 MHz): δ (ppm) = 7.93 (m, $^3J_{HH}$ = 8.7 Hz, 1H, H^9); 7.75 (m, 1H, H^6); 7.73 (d, $^3J_{HH}$ = 7.5 Hz, 1H, H^4); 7.72 (dd, $^3J_{HH}$ = 7.5 Hz, $^3J_{HP}$ = 5.1 Hz, 1H, H^1); 7.47 (dt, $^3J_{HH}$ = 7.5 Hz, $^4J_{HH}$ = 1.2 Hz, 1H, H^3); 7.41 (dt, $^3J_{HH}$ = 8.3 Hz, $^3J_{HP}$ = 1.6 Hz, 2H, *o*-Ph*H*); 7.36 (m, 2H; H^7, H^8); 7.32 (dt, $^3J_{HH}$ = 7.5 Hz, $^4J_{HP}$ = 2.5 Hz, 1H, H^2); 7.31 (m, 1H, *p*-Ph*H*); 7.27 (t, $^3J_{HH}$ = 7.2 Hz, 2H, *m*-Ph*H*). ^{13}C NMR ($CDCl_3$; 100.62 MHz): δ (ppm) = 148.2 (d, $^2J_{CP}$ = 3.8 Hz, C^{4b}); 145.9 (d, $^2J_{CP}$ = 4.2 Hz, C^{4a}); 142.9 (d, $^1J_{CP}$ = 4.2 Hz, C^{9b}); 139.5 (d, $^1J_{CP}$ = 2.2 Hz, C^{10a}); 138.1 (d, $^2J_{CP}$ = 8.1 Hz, C^{9a}); 138.0 (d, $^3J_{CP}$ = 17.0 Hz, C^{5a}); 133.8 (d, $^1J_{CP}$ = 16.9 Hz, *ipso*-PhP); 132.7 (d, $^2J_{CP}$ = 20.9 Hz, *o*-PhP); 130.1 (d, $^2J_{CP}$ = 21.5 Hz, C^1); 129.4 (d, $^4J_{CP}$ = 0.7 Hz, *p*-PhP); 128.7 (d, $^3J_{CP}$ = 7.8 Hz, *m*-PhP); 128.6 (s, C^3); 126.7 (d, $^3J_{CP}$ = 6.2 Hz, C^2); 124.9 (s, C^7); 124.4 (s, C^8); 123.5 (s, C^9); 122.9 (s, C^6); 121.6 (s, C^4). ^{31}P NMR ($CDCl_3$; 161.98 MHz): δ (ppm) = −17.4 (s). HR-MS (FAB): calcd for $C_{20}H_{14}PS$ (M + H): 317.0554, found: 317.0554. *m*/*z* (%): 317 (43) [M + H]$^+$, 316 (49) [M]$^+$, 239 (100) [M − Ph]$^+$. UV−vis (DCM): λ (nm) = 230 ($\varepsilon = 4.75 \times 10^4$ M^{-1} cm^{-1}); 260 ($\varepsilon = 2.93 \times 10^4$ M^{-1} cm^{-1}); 316 ($\varepsilon = 1.80 \times 10^4$ M^{-1} cm^{-1}); 340 (sh, $\varepsilon = 1.21 \times 10^4$ M^{-1} cm^{-1}). FS (cHex): λ (nm) = 411; Φ_F = 0.253.

10-Mesityl-10*H*-benzo[*b*]phosphindolo[2,3-*d*]thiophene (6b). *n*-BuLi (1.6 M in hexane, 700 μL, 1.12 mmol, 2.2 equiv) was added dropwise over a period of 30 min to a solution of 3-bromo-2-(2-bromophenyl)benzo[*b*]thiophene (185 mg, 503 μmol, 1 equiv) in Et_2O (10 mL) at −78 °C. The reaction mixture was stirred for 30 min at −78 °C and was then slowly warmed to room temperature over a period of 1.5 h. $MesPCl_2$ (111 mg, 503 μmol, 1 equiv) was slowly added dropwise to the light yellow turbid reaction mixture over a period of 20 min. Stirring was continued for 3 h, during which the reaction mixture turned slightly darker. The solvent was removed in vacuo, and the residue was extracted into Et_2O. After removal of the solvent in vacuo, the crude product was subjected to column chromatography over Al_2O_3 eluting with hexane and subsequently with hexane/DCM 1/1 (R_F (hexane) = 0.35), which afforded **6b** as a white solid (143 mg, 398 μmol, 79%). ^{1}H NMR ($CDCl_3$; 400.13 MHz): δ (ppm) = 7.89 (d, $^3J_{HH}$ = 7.2 Hz, 1H, H^9); 7.74 (d, $^3J_{HH}$ = 8.0 Hz, 1H, H^6); 7.64 (dd, $^3J_{HH}$ = 7.2 Hz, $^3J_{HP}$ = 4.8 Hz, 1H, H^1); 7.52 (dd, $^3J_{HH}$ = 7.2 Hz, $^4J_{HH}$ = 2.0 Hz, 1H, H^4); 7.44 (t, $^3J_{HH}$ = 7.2 Hz, 1H, H^3); 7.26−7.32 (m, 3H, H^2, H^7, H^8); 7.05 (bs, 1H, *m*-Mes*H*); 6.62 (bs, 1H, *m*-Mes*H*); 3.07 (bs, 3H, *o*-CH_3-ArP); 2.25 (s, 3H, *p*-CH_3-ArP); 1.26 (bs, 3H, *o*-CH_3-ArP). ^{13}C NMR ($CDCl_3$; 100.62 MHz): δ (ppm) = 145.1−145.3 (m, C^{4a}, C^{4b}, 2x *o*-ArP); 142.8 (d, $^1J_{CP}$ = 5.2 Hz, C^{9b}); 140.5 (d, $^4J_{CP}$ = 1.5 Hz, *p*-ArP); 139.1 (d, $^1J_{CP}$ = 5.4 Hz, C^{10a}); 138.3 (d, $^2J_{CP}$ = 8.0 Hz, C^{9a}); 137.9 (d, $^3J_{CP}$ = 17.1 Hz, C^{5a}); 130.0 (bs, *m*-ArP); 129.5 (d, $^2J_{CP}$ = 20.6 Hz, C^1); 127.6 (s, C^3); 125.9 (d, $^3J_{CP}$ = 8.0 Hz, C^2); 124.6 (s, C^7); 124.3 (s, C^8); 123.4 (s, C^9); 122.8 (s, C^6); 121.8 (s, C^4); 20.9 (s, *p*-CH_3−ArP), 18.9 (bs, *o*-CH_3−ArP), 13.9 (d, $^3J_{CP}$ = 20.2 Hz, *o*-CH_3−ArP). The signal for *ipso*-ArP is unresolved. ^{31}P NMR ($CDCl_3$; 161.98 MHz): δ (ppm) = −29.7 (s). HR-MS (FAB): calcd for $C_{23}H_{20}PS$ (M + H): 359.1023, found: 359.1024. *m*/*z* (%): 359 (75) [M + H]$^+$, 358 (91) [M]$^+$, 239 (100) [M − Mes]$^+$. UV−vis (DCM): λ (nm) = 236 ($\varepsilon = 9.40 \times 10^4$ M^{-1} cm^{-1}); 303 ($\varepsilon = 4.71 \times 10^4$ M^{-1} cm^{-1}); 310 ($\varepsilon = 4.64 \times 10^4$ M^{-1} cm^{-1}); 343 (sh, $\varepsilon = 2.13 \times 10^4$ M^{-1} cm^{-1}). FS (cHex): λ (nm) = 408 (Φ_F = 0.121).

10-(2,4,6-Triisopropylphenyl)-10*H*-benzo[*b*]phosphindolo-[2,3-*d*]thiophene (6c). *n*-BuLi (1.6 M in hexane, 1.60 mL, 2.55 mmol, 2.2 equiv) was added dropwise over a period of 30 min to a solution of 3-bromo-2-(2-bromophenyl)benzo[*b*]thiophene (426 mg, 1.16 mmol, 1 equiv) in Et_2O (23 mL) at −78 °C. The reaction mixture was stirred for 30 min at −78 °C and was then slowly warmed to room temperature over a period of 1.5 h. $IsPCl_2$ (0.35 M in Et_2O, 3.32 mL, 116 mmol, 1 equiv) was slowly added dropwise to the light yellow turbid reaction mixture over a period of 45 min. Stirring was continued for 16 h, during which the reaction mixture turned slightly darker. The solvent was removed in vacuo, and the residue was extracted into a mixture of Et_2O and DCM. After removal of the solvent in vacuo, the crude product was purified by column chromatography over Al_2O_3 eluting with hexane and subsequently with hexane/DCM 1/1 (R_F (hexane) = 0.31), which afforded **6c** as a yellow solid (516 mg, 1.16 mmol, 100%). ^{1}H NMR ($CDCl_3$; 400.13 MHz): δ (ppm) = 7.89 (d, $^3J_{HH}$ = 8.0 Hz, 1H, H^9); 7.81 (d, $^3J_{HH}$ = 7.8 Hz, 1H, H^6); 7.68 (dd, $^3J_{HH}$ = 7.5 Hz, $^3J_{HP}$ = 5.0 Hz, 1H, H^1); 7.55 (dd, $^3J_{HH}$ = 7.3 Hz, $^4J_{HH}$ = 1.7 Hz, 1H, H^4); 7.45 (t, $^3J_{HH}$ = 7.3 Hz, 1H, H^3); 7.32 (dt, $^3J_{HH}$ = 7.3 Hz, $^4J_{HH}$ = 1.7 Hz, 1H, H^2); 7.27−7.31 (m, 2H, H^7, H^8); 7.21 (dd, $^4J_{HP}$ = 5.6 Hz, $^4J_{HH}$ = 1.6 Hz, 1H, *m*-Is*H*); 6.82 (d, $^4J_{HH}$ = 1.6 Hz, 1H, *m*-Is*H*); 4.85 (sept, $^3J_{HH}$ = 6.8 Hz, 1H, *o*-$(CH_3)_2$-C*H*-ArP); 2.90 (sept, $^3J_{HH}$ = 6.8 Hz, 1H, *o*-$(CH_3)_2$C*H*-ArP); 1.91 (sept, $^3J_{HH}$ = 6.8 Hz, 1H, *p*-$(CH_3)_2$C*H*-ArP); 1.60 (d, $^3J_{HH}$ = 6.9 Hz, 3H, *o*-$(CH_3)_2$CH-ArP); 1.54 (d, $^3J_{HH}$ = 6.9 Hz, 3H, *o*-$(CH_3)_2$CH-ArP); 1.29 (d, $^3J_{HH}$ = 6.8 Hz, 6H, *p*-$(CH_3)_2$CH-ArP); 0.44 (d, $^3J_{HH}$ = 6.8 Hz, 3H, *o*-$(CH_3)_2$CH-ArP); 0.31 (d, $^3J_{HH}$ = 6.8 Hz, 3H, *o*-$(CH_3)_2$CH-ArP). ^{13}C NMR ($CDCl_3$; 100.62 MHz): δ (ppm) = 157.8 (d, $^2J_{CP}$ = 36.1 Hz, *o*-Is); 156.9 (d, $^2J_{CP}$ = 5.2 Hz, *o*-Is); 151.9 (d, $^4J_{CP}$ = 1.3 Hz, *p*-Is); 147.7 (d, $^2J_{CP}$ = 1.3 Hz, C^{4b}); 144.2 (d, $^2J_{CP}$ = 11.1 Hz, C^{4a}); 142.8 (d, $^1J_{CP}$ = 5.6 Hz, C^{9b}); 141.3 (d, $^1J_{CP}$ = 8.6 Hz, C^{10a}); 138.3 (d, $^2J_{CP}$ = 6.1 Hz, C^{9a}); 138.1 (d, $^3J_{CP}$ = 17.1 Hz, C^{5a}); 129.3 (d, $^2J_{CP}$ = 20.1 Hz, C^1); 127.4 (s, C^3); 125.5 (s, C^7); 124.7 (s, C^8); 124.3 (s, C^2); 123.5 (s, C^9); 122.9 (s, C^4); 122.70 (s, *m*-Is); 122.69 (d, $^1J_{CP}$ = 57.6 Hz, *ipso*-Is); 122.2 (s, C^6); 121.8 (d, $^3J_{CP}$ = 8.8 Hz,

dx.doi.org/10.1021/ic201116p |*Inorg. Chem.* 2011, 50, 8516–8523

m-Is); 34.2 (s, *p*-$(CH_3)_2$CH-ArP); 33.0 (d, $^3J_{CP}$ = 38.0 Hz, *o*-$(CH_3)_2$CH-ArP); 29.3 (s, *o*-$(CH_3)_2$CH-ArP); 25.4 (s, *o*-$(CH_3)_2$CH-ArP); 24.7 (s, *o*-$(CH_3)_2$CH-ArP); 23.9 (s, *o*-$(CH_3)_2$CH-ArP); 23.7 (s, *p*-$(CH_3)_2$CH-ArP); 23.3 (s, *o*-$(CH_3)_2$CH-ArP). ^{31}P NMR ($CDCl_3$; 161.98 MHz): δ (ppm) = −33.4 (s). HR-MS (FAB): calcd for $C_{29}H_{32}PS$: 443.1962 (M + H), found: 443.1960. *m*/*z* (%): 443 (73) $[M + H]^+$, 442 (100) $[M]^+$, 239 (44) $[M - Is]^+$. UV−vis (DCM): λ (nm) = 230 (ε = 4.55 × 10^4 M^{-1} cm^{-1}); 259 (ε = 2.99 × 10^4 M^{-1} cm^{-1}); 302 (ε = 2.00 × 10^4 M^{-1} cm^{-1}); 324 (ε = 1.66 × 10^4 M^{-1} cm^{-1}); 345 (sh, ε = 9.04 × 10^3 M^{-1} cm^{-1}). FS (cHex): λ (nm) = 409; Φ_F = 0.154.

10-Phenyl-10*H*-benzo[*b*]oxophosphindolo[2,3-*d*]thiophene (7a). H_2O_2 (44 μL, 1.80 mmol, 6 equiv) was added slowly to a solution of **6a** (94.9 mg, 300 μmol, 1 equiv) in DCM (10 mL). After 4 h of stirring, the reaction was complete, and a few drops of water were added to the reaction mixture. The solution was dried over $MgSO_4$, filtered, and the solvent was removed in vacuo. The yellowish residue was subjected to column chromatography over Al_2O_3 eluting with DCM and subsequently with DCM/MeOH (98/2) (R_F (DCM) = 0.05) to obtain **7a** as a white solid (46.6 mg, 140 μmol, 47%). Mp: 160.8−161.3 °C. ^{1}H NMR ($CDCl_3$; 400.13 MHz): δ (ppm) = 7.83−7.86 (m, $^3J_{HH}$ = 7.2 Hz, 1H, H^9); 7.78−7.81 (m, 1H, H^6); 7.73−7.78 (m, 2H, H^2, H^3); 7.67 (dd, $^3J_{HP}$ = 10.4 Hz, $^3J_{HH}$ = 7.2 Hz, 1H, H^1); 7.50−7.52 (m, 2H, *o*-PhH); 7.48 (dd, $^3J_{HH}$ = 7.2 Hz, $^4J_{HH}$ = 2.0 Hz, 1H, H^4); 7.35−7.41 (m, 2H, H^7, H^8); 7.29−7.34 (m, 3H, *m*-PhH, *p*-PhH). ^{13}C NMR ($CDCl_3$; 100.62 MHz): δ (ppm) = 154.5 (d, $^2J_{CP}$ = 18.1 Hz, C^{4b}); 143.1 (d, $^2J_{CP}$ = 12.1 Hz, C^{4a}); 137.4 (d, $^2J_{CP}$ = 19.1 Hz, C^{9a}); 136.6 (d, $^1J_{CP}$ = 101.6 Hz, C^{10a}); 136.0 (d, $^3J_{CP}$ = 5.0 Hz, C^{5a}); 133.0 (d, $^4J_{CP}$ = 2.0 Hz, *p*-PhP); 132.3 (d, $^2J_{CP}$ = 2.9 Hz, C^1); 130.8 (d, $^3J_{CP}$ = 11.2 Hz, *m*-PhP); 130.7 (d, $^1J_{CP}$ = 78.4 Hz, *ipso*-PhP); 129.6 (d, $^1J_{CP}$ = 108.9 Hz, C^{9b}); 129.4 (d, $^4J_{CP}$ = 4.2 Hz, C^3); 129.3 (d, $^3J_{CP}$ = 5.7 Hz, C^2); 128.8 (d, $^2J_{CP}$ = 12.9 Hz, *o*-PhP); 125.9 (s, C^7); 125.4 (s, C^8); 123.33 (s, C^9); 123.27 (s, C^6); 121.8 (d, $^3J_{CP}$ = 9.1 Hz, C^4). ^{31}P NMR ($CDCl_3$; 161.98 MHz): δ (ppm) = 25.5 (s). HR-MS (ESI): calcd for $C_{20}H_{13}OPSNa$ (M + Na): 355.0322, found: 355.0317. *m*/*z* (%): 355 (100) $[M + Na]^+$. IR (neat): ν (cm^{-1}) = 3391 (w); 3055 (w); 2920 (w); 2856 (w); 1589 (w); 1458 (w); 1435 (w); 1420 (w); 1312 (w); 1261 (w); 1192 (m); 1107 (m); 1022 (m); 790 (m); 748 (s); 721 (m); 709 (m); 690 (m); 633 (m); 524 (s); 428 (m). UV−vis (DCM): λ (nm) = 260 (ε = 1.73 × 10^4 M^{-1} cm^{-1}); 268 (sh, ε = 1.44 × 10^4 M^{-1} cm^{-1}); 302 (ε = 5.52 × 10^3 M^{-1} cm^{-1}); 330 (ε = 3.20 × 10^3 M^{-1} cm^{-1}); 352 (sh, ε = 2.77 × 10^3 M^{-1} cm^{-1}). FS (cHex): λ (nm) = 411; Φ_F = 0.837.

10-Mesityl-10*H*-benzo[*b*]oxophosphindolo[2,3-*d*]thiophene (7b). H_2O_2 (19 μL, 797 μmol, 6 equiv) was added slowly to a solution of **6b** (47.6 mg, 133 μmol, 1 equiv) in DCM (4 mL). After 6 h of stirring, the reaction was complete, and a few drops of water were added to the reaction mixture. The solution was dried over $MgSO_4$, filtered, and the solvent was removed in vacuo. The yellowish residue was subjected to column chromatography over Al_2O_3 eluting with DCM and subsequently with DCM/MeOH (95/5) (R_F (95/5) = 0.59) to obtain **7b** as a white solid (22.4 mg, 59.8 μmol, 45%). Mp: 110.3−112.5 °C. ^{1}H NMR ($CDCl_3$; 400.13 MHz): δ (ppm) = 7.85−788 (m, 1H, H^9); 7.68−7.72 (m, 1H, H^6); 7.64 (dd, $^3J_{HP}$ = 10.4 Hz, $^3J_{HH}$ = 7.2 Hz, 1H, H^1); 7.50−7.54 (m, 2H, H^3, H^4); 7.35 (dd, $^3J_{HH}$ = 7.34 Hz, $^4J_{HP}$ = 3.4 Hz, 1H, H^2); 7.31−7.35 (m, 2H, H^7, H^8); 6.88 (d, $^4J_{HP}$ = 3.6 Hz, 2H, *m*-MesH); 2.27 (s, 3H, *p*-CH_3-ArP); 1.43 (s, 3H, *o*-CH_3-ArP); 0.88 (s, 3H, *o*-CH_3-ArP). ^{13}C NMR ($CDCl_3$; 125.80 MHz): δ (ppm) = 154.0 (d, $^2J_{CP}$ = 26.2 Hz, C^{4b}); 143.2 (d, $^2J_{CP}$ = 12.1 Hz, C^{9a}); 142.04 (s, *p*-ArP or *o*-ArP); 142.02 (s, *p*-ArP or *o*-ArP); 138.4 (d, $^1J_{CP}$ = 107.3 Hz, C^{10a}); 137.4 (d, $^2J_{CP}$ = 18.0 Hz, C^{4a}); 136.1 (d, $^3J_{CP}$ = 13.0 Hz, C^{5a}); 132.7 (d, $^4J_{CP}$ = 2.1 Hz, C^3); 132.6 (d, $^1J_{CP}$ = 105.4 Hz, C^{9b}); 132.4 (s, *o*-ArP); 131.5 (d, $^3J_{CP}$ = 12.1 Hz, *m*-ArP); 129.5 (d, $^3J_{CP}$ = 11.2 Hz, C^2); 128.8 (d, $^2J_{CP}$ = 10.1 Hz, C^1); 125.9 (s, C^7); 125.3 (s, C^8); 123.43 (s, C^6); 123.41 (s, C^9); 122.1 (d, $^3J_{CP}$ = 8.7 Hz, C^4); 121.3 (d, $^1J_{CP}$ = 102.3 Hz, *ipso*-ArP); 30.3 (s, *o*-CH_3−ArP); 21.0 (s, *p*-CH_3−ArP); 14.1 (s, *o*-CH_3−ArP). ^{31}P NMR ($CDCl_3$; 161.98 MHz): δ (ppm) = 27.4 (s). HR-MS (ESI): calcd for $C_{23}H_{20}OPS$ (M + H): 375.0972, found: 375.0967. *m*/*z* (%): 375 (100) $[M + H]^+$. IR (neat): ν (cm^{-1}) = 3298 (w); 2959 (w); 2924 (w); 2855 (w); 1640 (w); 1412 (m); 1261 (m); 1018 (w); 872 (w); 799 (s); 694 (w); 451 (m). UV−vis (DCM): λ (nm) = 229 (sh, ε = 1.64 × 10^4 M^{-1} cm^{-1}); 257 (ε = 1.35 × 10^4 M^{-1} cm^{-1}); 269 (sh, ε = 9.96 × 10^3 M^{-1} cm^{-1}); 304 (ε = 4.44 × 10^3 M^{-1} cm^{-1}); 329 (ε = 3.33 × 10^3 M^{-1} cm^{-1}); 353 (sh, ε = 2.42 × 10^3 M^{-1} cm^{-1}). FS (cHex): λ (nm) = 409; Φ_F = 0.895.

10-(2,4,6-Triisopropylphenyl)-10*H*-benzo[*b*]oxophosphindolo[2,3-*d*]thiophene (7c). H_2O_2 (56 μL, 2.32 mmol, 6 equiv) was added slowly to a solution of **6c** (172 mg, 386 μmol, 1 equiv) in DCM (10 mL). After 16 h of stirring, the reaction was complete, and a few drops of water were added to the reaction mixture. The solution was dried over $MgSO_4$, filtered, and the solvent was removed in vacuo. The yellowish residue was subjected to column chromatography over Al_2O_3 eluting with DCM and subsequently with DCM/MeOH (95/5) (R_F (DCM) = 0.12) to obtain **7c** as a white solid (64.2 mg, 140 μmol, 36%). Mp: 112.6−113.1 °C. ^{1}H NMR ($CDCl_3$; 400.13 MHz): δ (ppm) = 7.84−7.87 (m, 1H, H^9); 7.68−7.73 (m, 1H, H^6); 7.64 (dd, $^3J_{HP}$ = 10.6 Hz, $^3J_{HH}$ = 7.4 Hz, 1H, H^1); 7.53 (dd, $^3J_{HH}$ = 7.4 Hz, $^4J_{HP}$ = 3.2 Hz, 1H, H^4); 7.49 (dd, $^3J_{HH}$ = 7.4 Hz, $^4J_{HH}$ = 1.3 Hz, 1H, H^3); 7.35 (ddd, $^3J_{HH}$ = 7.3 Hz, $^4J_{HP}$ = 3.7 Hz, $^4J_{HH}$ = 1.3 Hz, 1H, H^2); 7.29−7.33 (m, 2H, H^7, H^8); 7.11 (d, $^4J_{HP}$ = 4.0 Hz, 2H, *m*-IsH); 2.88 (sept, $^3J_{HH}$ = 6.9 Hz, 1H, *p*-$(CH_3)_2CH$-ArP); 1.16−1.34 (m, 2H, *o*-$(CH_3)_2CH$-ArP); 1.25 (dd, $^3J_{HH}$ = 6.9 Hz, 3H, *p*-$(CH_3)_2$CH-ArP); 1.02 (bd, $^3J_{HH}$ = 6.4 Hz, 3H, *o*-$(CH_3)_2$CH-ArP); 0.93 (bd, $^3J_{HH}$ = 6.4 Hz, 3H, *o*-$(CH_3)_2$CH-ArP). ^{13}C NMR ($CDCl_3$; 100.62 MHz): δ (ppm) = 152.8 (d, $^4J_{CP}$ = 2.8 Hz, *p*-Is); 152.6 (d, $^2J_{CP}$ = 25.4 Hz, C^{4b}); 147.7 (s, *o*-Is); 143.2 (d, $^2J_{CP}$ = 11.8 Hz, C^{9a}); 140.3 (d, $^1J_{CP}$ = 107.7 Hz, C^{10a}); 138.7 (s, *o*-Is); 136.7 (d, $^2J_{CP}$ = 17.4 Hz, C^{4a}); 136.1 (d, $^3J_{CP}$ = 13.0 Hz, C^{5a}); 134.8 (d, $^1J_{CP}$ = 105.0 Hz, C^{9b}); 132.4 (d, $^4J_{CP}$ = 2.0 Hz, C^3); 129.3 (d, $^3J_{CP}$ = 11.3 Hz, C^2); 128.5 (d, $^2J_{CP}$ = 10.2 Hz, C^1); 125.8 (s, C^7); 125.2 (s, C^8); 123.38 (s, C^9); 123.35 (s, *m*-Is); 123.26 (s, C^6); 122.2 (d, $^3J_{CP}$ = 8.7 Hz, C^4); 119.0 (d, $^1J_{CP}$ = 102.4 Hz, *ipso*-Is); 34.1 (s, *p*-$(CH_3)_2$CH-ArP); 30.1 (s, *o*-$(CH_3)_2$CH-ArP); 30.0 (s, *o*-$(CH_3)_2$CH-ArP); 24.9 (bs, *o*-$(CH_3)_2$CH-ArP); 24.5 (bs, *o*-$(CH_3)_2$-CH-ArP); 23.6 (s, *p*-$(CH_3)_2$CH-ArP). ^{31}P NMR ($CDCl_3$; 161.98 MHz): δ (ppm) = 28.1 (s). HR-MS (FAB): calcd for $C_{29}H_{32}OPS$ (M + H): 459.1911, found: 459.1909. *m*/*z* (%): 459 (100) $[M + H]^+$, 255 (18) $[M - Is]^+$, 239 (11) $[M - OIs]^+$. IR (neat): ν (cm^{-1}) = 2959 (w); 2924 (w); 2866 (w); 1601 (w); 1462 (w); 1416 (w); 1312 (w); 1261 (m); 1184 (m); 1072 (s); 1018 (s); 941 (w); 880 (w); 795 (s); 752 (s); 718 (m); 675 (m); 648 (m); 521 (s); 490 (m); 451 (m). UV−vis (DCM): λ (nm) = 233 (ε = 2.49 × 10^4 M^{-1} cm^{-1}); 264 (ε = 2.76 × 10^4 M^{-1} cm^{-1}); 271 (sh, ε = 2.45 × 10^4 M^{-1} cm^{-1}); 329 (ε = 4.92 × 10^3 M^{-1} cm^{-1}); 364 (sh, ε = 2.57 × 10^3 M^{-1} cm^{-1}). FS (cHex): λ (nm) = 408; Φ_F = 0.683.

■ ASSOCIATED CONTENT

Supporting Information. An extensive description of the computational results for **6** and the calibration line, including frontier orbital pictures and coordinates. This material is available free of charge via the Internet at http://pubs.acs.org.

■ AUTHOR INFORMATION

Corresponding Author
*E-mail: k.lammertsma@vu.nl.

■ ACKNOWLEDGMENT

This work benefitted from interactions within the European PhoSciNet (CM0802).

REFERENCES

(1) (a) Baumgartner, T.; Réau, R. *Chem. Rev.* **2006**, *106*, 4681–4727. (b) Hissler, M.; Lescop, C.; Réau, R. *J. Organomet. Chem.* **2005**, *690*, 2482–2487. (c) Hissler, M.; Dyer, P. W.; Réau, R. *Top. Cur. Chem.* **2005**, *250*, 127–163.

(2) (a) Hobbs, M. G.; Baumgartner, T. *Eur. J. Inorg. Chem.* **2007**, 3611–3628. (b) Hissler, M.; Lescop, C.; Reau, R. *C. R. Chim.* **2008**, *11*, 628–640. (c) Matano, Y.; Imahori, H. *Org. Biomol. Chem.* **2009**, *7*, 1258–1271.

(3) Su, H. C.; Fadhel, O.; Yang, C. J.; Chio, T. Y.; Fave, C.; Hissler, M.; Wu, C. C.; Réau, R. *J. Am. Chem. Soc.* **2006**, *128*, 983–995.

(4) Mathey, F. *Chem. Rev.* **1988**, *88*, 429–453.

(5) (a) Baumgartner, T.; Neumann, T.; Wirges, B. *Angew. Chem., Int. Ed.* **2004**, *43*, 6197–6201. (b) Dienes, Y.; Durben, S.; Kárpáti, T.; Neumann, T.; Englert, U.; Nyulaszi, L.; Baumgartner, T. *Chem.—Eur. J.* **2007**, *13*, 7487–7500.

(6) (a) Fukazawa, A.; Hara, M.; Okamoto, T.; Son, E. C.; Xu, C.; Tamao, K.; Yamaguchi, S. *Org. Lett.* **2008**, *10*, 913–916. (b) Fukazawa, A.; Yamada, H.; Yamaguchi, S. *Angew. Chem., Int. Ed.* **2008**, *47*, 5582–5585. (c) Fukazawa, A.; Ichihashi, Y.; Kosaka, Y.; Yamaguchi, S. *Chem.—Asian J.* **2009**, *4*, 1729–1740.

(7) See for example: Turro, N. J. In *Modern Molecular Photochemistry*, Section 5.7 Experimental Measurements of the Absorption and Emission of Light: Molecular Electronic Spectroscopy; University Science Books: Sausalito, CA, 1991; pp 110−111.

(8) Ren, Y.; Baumgartner, T. *J. Am. Chem. Soc.* **2011**, *133*, 1328–1340.

(9) (a) Keglevich, G.; Böcskei, Z.; Keserü, G. M.; Újszászy, K.; Quin, L. D. *J. Am. Chem. Soc.* **1997**, *119*, 5095–5099. (b) Keglevich, G.; Quin, L. D.; Böcskei, Z.; Keserü, G. M.; Kalgutkar, R.; Lahti, P. M. *J. Organomet. Chem.* **1997**, *532*, 109–116.

(10) Wittig, G.; Maercker, A. *Chem. Ber.* **1964**, *97*, 747–768.

(11) (a) Dore, A.; Fabbri, D.; Gladialia, S.; De Lucchib, O. *J. Chem. Soc., Chem. Commun.* **1993**, 1124–1125. (b) Leroux, F.; Mangano, G.; Schlosser, M. *Eur. J. Org. Chem.* **2005**, 5049–5054. (c) Dubrovina, N. V.; Jiao, H.; Tararov, V. I.; Spannenberg, A.; Kadyrov, R.; Monsees, A.; Christiansen, A.; Börner, A. *Eur. J. Org. Chem.* **2006**, 3412–3420. (d) Geramita, K.; McBee, J.; Tilley, T. D. *J. Org. Chem.* **2009**, *74*, 820–829. (e) Dienes, Y.; Eggenstein, M.; Kárpáti, T.; Sutherland, T. C.; Nyulászi, L.; Baumgartner, T. *Chem.—Eur. J.* **2008**, *14*, 9878–9889. (f) Ren, Y.; Dienes, Y.; Hettel, S.; Parvez, M.; Hoge, B.; Baumgartner, T. *Organometallics* **2009**, *28*, 734–740. (g) Baumgartner, T.; Wilk, W. *Org. Lett.* **2006**, *8*, 503–506.

(12) Heynderickx, A.; Samat, A.; Guglielmetti, R. *Synthesis* **2002**, 213–216.

(13) Unfortunately, the supermesityl (2,4,6-tritertbutylphenyl) substituted analogue could not be prepared according to this procedure, probably because of too high steric congestion around the phosphorus centre.

(14) Chesnut, D. B.; Quin, L. D. *J. Am. Chem. Soc.* **1994**, *116*, 9638–9643.

(15) Keglevich, G.; Quin, L. D.; Böcskei, Z.; Keserü, G. M.; Kalgutkar, R.; Lahti, P. M. *J. Organomet, Chem.* **1997**, *532*, 109–116.

(16) A detailed description of the calibration curve of constrained analogues of **6a** is given in the Supporting Information.

(17) Because of difficult chromatographic purification, yields are lower than similar phosphole oxidations (cf. 85% for **2** (R = $SiHMe_2$)).[13]

(18) *ADF 2008.01*; SCM, Theoretical Chemistry, VU University: Amsterdam, The Netherlands, 2008; http://www.scm.com/.

(19) Becker, G.; Mundt, O.; Rössler, M.; Schneider, E. *Z. Anorg. Allg. Chem.* **1978**, *443*, 42–52.

(20) Chandrasekhar, V.; Sasikumar, P.; Boomishankar, R.; Anantharaman, G. *Inorg. Chem.* **2006**, *45*, 3344–3351.

(21) Barbarella, G.; Favaretto, L.; Zanelli, A.; Gigli, G.; Mazzeo, M.; Anni, M.; Bongini, A. *Adv. Funct. Mater.* **2005**, *15*, 664–670.